# Partitioning of Membrane-Anchored DNA between Coexisting Lipid Phases[†]

## Paul A. Beales[‡,§] and T. Kyle Vanderlick*,[§]

*Department of Chemical Engineering, Princeton University, Princeton, New Jersey 08544, and Department of Chemical Engineering, Yale University, New Haven, Connecticut 06511*

*Received: January 22, 2009; Revised Manuscript Received: April 13, 2009*

The partitioning of different cholesterol-modified single-stranded DNA molecules (chol-DNAs) between the domains of phase-separated lipid vesicles is investigated by laser-scanning confocal fluorescence microscopy. All chol-DNAs studied preferentially localized into the fluid phase of giant vesicles in liquid−solid phase coexistence (1:1 DLPC:DPPC, 1:1 DLPC:DMPE). Partitioning behavior of chol-DNAs into liquid−liquid phase-separated vesicles (DOPC/DPPC/cholesterol) was found to be less straightforward. Single-cholesterol-anchored DNA molecules partitioned roughly equally between coexisting domains, whereas chol-DNAs with two cholesterol anchors were seen to be enriched in the liquid-ordered domains with apparent surface concentrations up to double that of the liquid-disordered phase. Quantitative analysis of the fluorescence intensity of DNA between the two phases also revealed a weaker dependence of the apparent partitioning on the initial lipid composition of the vesicles. We rationalize these observations by proposing a simple partitioning model based on the conformational entropy of insertion of a cholesterol anchor into each phase.

## Introduction

DNA is a digital, information-carrying molecule by nature's design that is attracting much interest for applications in bionanotechnology.[1] Lipid structures, e.g., vesicles, also attract much technological development as soft, biocompatible containers for molecular isolation and delivery. Encoding the surface of these liposomal capsules with information by functionalizing the membrane with nucleic acid sequences in order to fabricate "smart" containers has wide-ranging scientific and technological appeal. Indeed, recent reports have highlighted the utility of nucleic acid strands modified with hydrophobic moieties as tools in biotechnological applications.[2−26] DNA strands with hydrophobic modifications have also been used as model systems for biological membrane-bound receptors[27−29] and membrane fusion machinery.[30−32] The hydrophobic modifications preferentially associate with lipid bilayers, anchoring the DNA strands to reconstituted membrane structures such as lipid vesicles or solid-supported membranes. The anchored DNA is then free to bind to its complement by the well-known Watson−Crick base pair interactions, allowing the engineering of components that will bind with high specificity via their complementary target sequences.

Membrane-anchored DNA molecules will also allow the amalgamation between lipid bilayers and DNA nanostructures[33,34] and nanomachines.[35] The fluid nature of the lipid membrane would provide a two-dimensional substrate upon which anchored DNA structures and machines can interact. Current examples of DNA nanotechnology include molecular switches,[36−39] tweezers,[40,41] and DNA walkers.[42−44] Some future DNA nanotechnology applications may encompass membrane-anchored nanomachines that function in ways that take inspiration from the roles of membrane proteins in regulating cellular processes at its interface with the extracellular environment. Membrane-anchored DNA molecules could also be employed as aptamers. Nucleic acid aptamers are oligonucleotides which fold into 3D structures that bind with high specificity and high affinity to target molecules.[45,46] Anchored DNA aptamers could have applications in areas such as ligand-targeted drug delivery systems[47−51] or molecular detection assays.

Structural heterogeneity can offer added functionality to engineered materials. Membrane heterogeneities can be created by phase separation of coexisting lipid phases. Studies of simple (when compared to the complexity of natural biomembranes) two and three lipid component membranes have demonstrated the coexistence of fluid and solid-like lipid phases[52−58] as well as two coexisting liquid phases referred to as liquid-ordered and liquid-disordered phases, respectively.[59−62] The coexistence of two distinct surface characteristics in these membranes offers the possibility of engineering domains with distinct operational attributes that would allow the exploitation of designed bifunctionality of these lipid structures.

Chemically anisotropic particles on nanoscopic and microscopic length scales have attracted much recent interest, since such entities can have directional interactions that can be exploited to assemble a richer array of structural morphologies[63,64] and they can also be used to fabricate objects that exhibit autonomous motion.[65] In these respects, anisotropic, functional lipid vesicles could be engineered to assemble complex superstructures of vesicle containers encapsulating different chemical species or as proto-cellular models that exhibit a primitive mode of chemotaxis.

Coexisting lipid phases are also considered to be minimal model systems for heterogeneities in natural biomembranes, often referred to as "lipid rafts".[66−69] These *in vivo* lipid domains are considered to be important for cell signaling processes, preferentially recruiting or excluding receptors and other membrane inclusions.[70−72] Since membrane-anchored DNA has been considered as a minimal model for membrane-bound receptors and vesicle fusion machinery, clustering and local confinement of these molecules into lipid domains in vesicle membranes could prove to be a useful tool in exploring potential

Lipid Phase Partitioning of Anchored DNA

*J. Phys. Chem. B, Vol. 113, No. 42, 2009* **13679**

physiological roles of grouping receptors into spatially localized patches of the membrane. For example, increased local concentrations of membrane receptors by clustering into domains is thought to increase the binding affinity of individually weak ligand−receptor bonds.[73]

With these motivations in mind, we use fluorescence confocal microscopy to investigate the partitioning of DNA with hydrophobic modifications between coexisting lipid phases. We investigate the effect of the choice of membrane-anchoring geometry on DNA localization in giant vesicles with domains of solid-like phases ($L_\beta$ or $P_{\beta'}$) within a fluid ($L_\alpha$) matrix as well as membranes in liquid-ordered ($L_o$)−liquid-disordered ($L_\alpha$) coexistence (note that the liquid-disordered phase is also commonly denoted $L_d$ in the literature). The hydrophobic anchors we investigate in this work are all based on commercially available cholesteryl modifications, since their current ease of availability makes them the most accessible for wide use in scientific and engineering applications without the need for specialist skills in synthetic chemistry and DNA synthesis.

## Methods

**Materials.** The lipids 1,2-dilauroyl-*sn*-glycero-3-phosphocholine (DLPC), 1,2-dipalmitoyl-*sn*-glycero-3-phosphocholine (DPPC), 1,2-dioleoyl-*sn*-glycero-3-phosphocholine (DOPC), 1,2-dimyristoyl-*sn*-glycero-3-phosphoethanolamine (DMPE), and cholesterol (chol) were purchased from Avanti Polar Lipids. The lipophilic fluorophores Lissamine rhodamine B 1,2-dihexadecanoyl-*sn*-glycero-3-phosphoethanolamine, triethylammonium salt (Rh-DPPE) and 2-(4,4-difluoro-5,7-dimethyl-4-bora-3a,4a-diaza-*s*-indacene-3-pentanoyl)-1-hexadecanoyl-*sn*-glycero-3-phosphocholine (Bodipy-PC) were purchased from Invitrogen Molecular Probes. Cholesterol-modified oligonucleotides (chol-DNA) cholesteryl-TEG-5′-ACAGACTACC-3′ (chol-DNA-10A), cholesteryl-TEG-3′-TTTGGCCCGCGCCCCGCCCC-5′ (chol-DNA-20), cholesteryl-TEG-5′-TTTCCGGGCGCGGGGCG-GGGACAGACTACC-3′ (chol-DNA-30A), and parallel-cholesteryl-TEG-cholesteryl-TEG-5′-ACAGACTACC-3′ (2p-chol-DNA-10A) were purchased from Eurogentec North America and had been purified by HPLC. Fluorescently labeled DNA Alexa Fluor 647-5′-GGTAGTCTGT-3′ (A647-DNA-10B) was purchased from IDT and had also undergone HPLC purification.

**Vesicle Preparation.** Giant unilamellar vesicles (GUVs) were formed by electroformation. Lipid stock solutions in chloroform were made up at the desired molar ratio to a total lipid concentration of 1.0 mM. A 70 $\mu$L portion of lipid in chloroform solution was placed dropwise onto the platinum wires of the electroformation chamber and dried under a vacuum for at least 4 h. A preheated 300 mM aqueous sucrose solution was added to the electroformation chamber in an oven at a temperature in excess of 50 °C such that all lipids were in the fluid phase. A 3.0 V ac field was applied across the platinum wires at 10 Hz for 30 min, 3.0 Hz for 15 min, 1.0 Hz for 7 min, and 0.5 Hz for 7 min. The vesicles were then removed from the chamber. Chol-DNA dissolved in 125 mM NaCl, 10 mM Hepes (pH 7.4) was added to the GUV solution at a DNA:lipid ratio of <0.01; 163 mM NaCl, 10 mM Hepes (pH 7.4) was also added to the solution to give a final NaCl concentration of 110 mM. Either the addition of these solutions was done prior to phase separation at 50 °C, and this temperature was maintained for at least 30 min to allow chol-DNA to diffuse into the membranes before cooling, or the addition of these solutions was done after cooling to room temperature, i.e., after lipid phase separation, where the samples were again left for 30 min to ensure membrane association of the chol-DNA. Once samples had cooled to room

temperature and chol-DNA was incorporated in the vesicles, a solution of A647-DNA-10B was added at a 1:1 ratio with chol-DNA; the samples were left for a minimum of 30 min to allow the fluorescently labeled DNA to hybridize with the membrane-anchored DNA before imaging.

**Confocal Microscopy.** GUVs were imaged using the Leica TCS SP5 confocal system equipped with a Leica 63×/1.3 N.A. Plan Apo DIC Glycerin immersion objective lens. The Rh-DPPE probe was excited by a DPSS laser at 561 nm, the Bodipy-PC probe was excited with the 488 nm line of an argon laser, and the Alexa Fluor 647 was excited by a helium−neon laser at 633 nm. The photomultiplier tubes were offset such that the black level was zero across most of the sample before beginning experiments; variations in black level were, at worst, ±2 au across the image. Glass bottom culture dishes (MatTek Corporation, part no. P35G-1.5-20-C) were treated with a 10% Bovine Serum Albumin (Sigma) solution prior to use in order to prevent the vesicles from adhering to the glass coverslip. All vesicles were imaged at room temperature, approximately 21 ± 1 °C.

## Results and Discussion

We investigate the partitioning of three different chol-modified DNAs between coexisting lipid membrane phases. The three molecular geometries under investigation are shown in Figure 1. First, there is a single-chol-modified DNA (chol-DNA-10A). Second, there are two single-chol-modified DNAs (chol-DNA-20/chol-DNA-30A) where the chol-DNA-20 hybridizes to what will be the membrane-proximal portion of the chol-DNA-30A leaving an overlapping section of the chol-DNA-30A which can bind to complementary target sequences. This hybridized DNA pair results in a molecule with double-chol anchoring into lipid membranes, increasing the strength of membrane binding for longer DNA sequences. Finally, we test a double-chol-modified DNA (2p-chol-DNA-10A), where the two chol moieties are positioned parallel to one another by a symmetric spacer modification on the 5′ end of the DNA strand.

We study the partitioning of chol-DNA-10A and chol-DNA-20/chol-DNA-30A in vesicles exhibiting solid−fluid phase coexistence and the partitioning of all three chol-modified DNA geometries in vesicles in liquid−liquid phase coexistence. We directly visualize the chol-DNA partitioning in the vesicle membranes by confocal fluorescence microscopy which yields thin image sections through the vesicles highlighting the locations of fluorescent probes within the lipid membrane. Fluorescent lipids are used to mark the locations of the different lipid phases, while a water-soluble, fluorescent DNA (A647-DNA-10B) which is complementary to the chol-DNAs is added to the samples to elucidate the partitioning of the membrane-bound nucleic acids. This fluorescent DNA binds specifically to the chol-DNA, and the distribution of its fluorescence signal within the membrane can be resolved by the confocal microscope (see Figure 2). Note that control experiments where the fluorescent DNA was added to samples of GUVs that were not functionalized by chol-DNAs did not detect any nonspecific binding of the A647-DNA-10B to the membranes. Image sections obtained by confocal microscopy can be reconstructed to reveal the vesicle surface textures created by phase separation.

**Fluid−Solid Phase-Separated Vesicles.** The partitioning of chol-modified DNAs in 1:1 DLPC:DPPC giant unilamellar vesicles (GUVs) at room temperature was investigated. These vesicles contain coexisting $L_\alpha$ fluid and $P_{\beta'}$ solid phases. The $P_{\beta'}$ phase forms stripe-like domains templated by the anisotropic line tension of the corrugated ripples of the molecular-scale structure of this phase (Figure 3A,B):[55,56] in these images, the
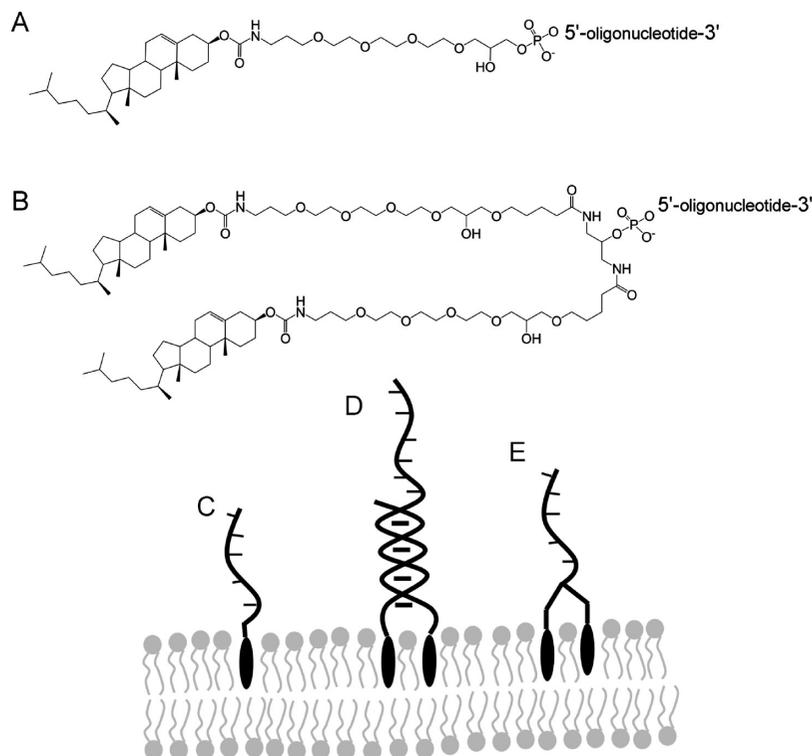
**Figure 1.** Chol-modified DNA structures: (A) chemical structure of a single-chol modification for a single-stranded DNA (ssDNA) molecule (DNA chemical structure is not drawn); (B) chemical structure of a double-chol modification for ssDNA molecules (two cholesteryl TEG molecules linked by a symmetric branched modification); (C) cartoon of single-chol-modified ssDNA anchoring the DNA molecule to a lipid bilayer (e.g., chol-DNA-10A); (D) cartoon of two single-chol-modified ssDNA molecules that hybridize together to create a double-chol anchor, leaving an overlapping sequence that is free to bind complementary targets (e.g., chol-DNA-20/chol-DNA-30A); (E) cartoon of a double-chol-modified ssDNA anchored to a lipid membrane (e.g., 2p-chol-DNA-10A).

Bodipy-PC dye (green) partitions preferentially into the fluid phase and Rh-DPPE (red) enriches in the solid-like $P_{\beta'}$ phase. Figure 3C−F shows single confocal sections through the equator of these vesicles where A647-DNA-10B (blue), and hence the chol-DNA, is observed to have localized preferentially to the fluid $L_\alpha$ regions of the membrane. The chol-DNA (single-chol-anchored chol-DNA-10A or double-chol-anchored chol-DNA-20/chol-DNA-30A) was always observed to partition preferentially into the fluid phase of these vesicles regardless of whether the vesicles were functionalized with chol-DNA before or after the membrane phase separated; i.e., no history dependence was observed in the chol-DNA partitioning.

We also investigated the partitioning of chol-DNA in fluid−solid phase-separated vesicles where the solid-like phase has a flat, lamellar structure as opposed to the rippled structure of the $P_{\beta'}$ phase. 1:1 DLPC:DMPE vesicles phase separate into coexisting $L_\alpha$ fluid and $L_\beta$ solid-like phases. The $L_\beta$ phase is thought to have no long-range molecular ordering on optically resolvable length scales. On slow cooling, these domains form circular domains which ripen by limited coalescence due to the slow molecular diffusion in the solid-like phase on experimental time scales, upon which further domain growth occurs.[54−56] This results in surface textures exemplified in Figure 4A1, B1, C1, and D1; these images show the morphologies of vesicle hemispheres that have been reconstructed from the confocal image slices. In these images, Rh-DPPE (red) partitions into the fluid phase, leaving the $L_\beta$ solid phase to appear dark. Figure 4A2, B2, C2, and D1 reveals the partitioning of chol-DNA between the fluid and solid-like phases. As in the previous case of DLPC/DPPC vesicles, both the single-anchored chol-DNA-10A and the double-anchored chol-DNA-20/chol-DNA-30A were preferentially found to be located in the $L_\alpha$ fluid phase;

no significant fluorescent signal from the A647-chol-10B could be detected in the solid-like $L_\beta$ domains. This preference of the chol-DNA partitioning was not affected by the addition of the chol-DNA prior to or after phase separation in the vesicle's membrane in sample preparation.

The single- and double-chol anchoring of DNA to lipid membranes in solid−fluid phase coexistence always resulted in the DNA functionality partitioning into the fluid phase of the systems that we investigated. This comes as little surprise, since impurities are normally expected to partition into the less ordered of the two phases, since it is rare for molecular additives to have a lower free energy cost by inserting into phases with a higher molecular ordering, e.g., the enrichment of Rh-DPPE in the $P_{\beta'}$ phase of vesicles in $L_\alpha−P_{\beta'}$ coexistence. However, these systems do demonstrate that asymmetric distributions of membrane-anchored DNA can easily be fabricated by engineering the lipid composition such that the membrane phase separates into coexisting fluid and solid-like phases. Furthermore, by selection of the particular solid-like lipid phase that forms, different domain morphologies are attainable: therefore, this allows a degree of control over the resulting texture of the DNA surface distribution.

While an asymmetric distribution of membrane-anchored DNA is attainable by solid−liquid phase separation, these systems may have limitations depending on the intended application. For example, it would be difficult to find a second hydrophobic anchor that would partition into the solid domains in order to anchor a second DNA sequence in the opposite domains to create bifunctionalized vesicles. Furthermore, solid domains place certain restrictions on the resultant morphological distribution of domains. Therefore, we study the partitioning

Lipid Phase Partitioning of Anchored DNA

*J. Phys. Chem. B, Vol. 113, No. 42, 2009* **13681**
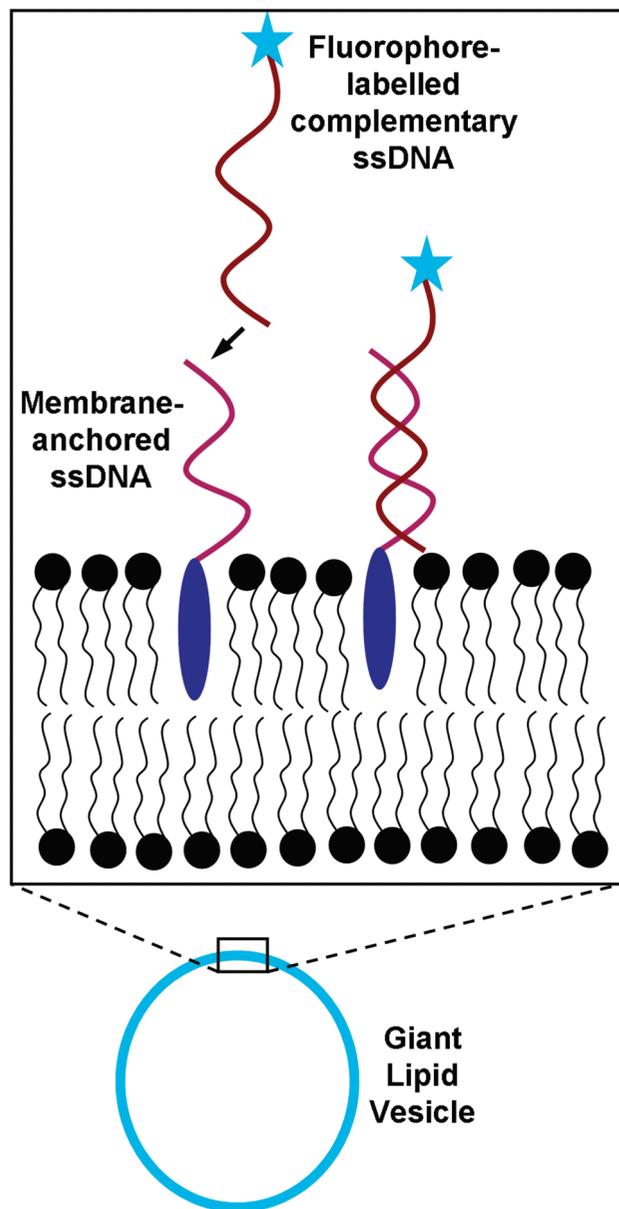


**Figure 2.** Cartoon of the experimental setup. The partitioning or membrane-anchored DNA is visualized by observing where on the membrane a fluorescently labeled complementary strand binds.



**Figure 3.** Giant vesicles in $L_\alpha$–$P_{\beta'}$ phase coexistence. Red represents Rh-DPPE (the $P_{\beta'}$ phase), green represents Bodipy-PC (the $L_\alpha$ phase), and blue represents Alexa-647 (DNA). (A, B) Reconstructions of vesicle hemispheres demonstrating the characteristic stripe morphology of ripple phase domains in GUVs. (C, D) Single confocal slices through the equator of a vesicle: (C) lipid phase probes; (D) DNA probe. (E, F) Single confocal slices through the equator of a vesicle that has been deformed from its native spherical geometry by the growth of the solid-like ripple phase domains: (E) lipid phase probes; (F) DNA probe. All vesicles are 1:1 DLPC:DPPC at 21 ± 1 °C.

of chol-DNAs between coexisting liquid phases to investigate whether such systems might overcome some of these limitations.

**Liquid–Liquid Phase-Separated Vesicles.** Ternary vesicles composed of a saturated lipid, an unsaturated lipid, and cholesterol can phase separate into coexisting liquid phases, e.g., DOPC/DPPC/chol.[61,62] Deuterium NMR studies of this system reveal the thermodynamic tie lines along which the membranes phase separate and show that the liquid-ordered phase ($L_o$) is rich in DPPC and chol and the liquid-disordered phase ($L_\alpha$) is rich in DOPC and has a lower chol composition.[74] A first order assumption might be that the cholesteryl moieties of the chol-DNA molecules will therefore enrich in the $L_o$ phase of these vesicles. However, it is well established that probes designed as cholesterol mimics usually do not satisfactorily reproduce the properties of pure cholesterol.[75,76] Small changes to the structure of cholesterol can have a significant influence on the properties, composition, and location in phase space of coexisting lipid domains, as has been demonstrated by experiments where cholesterol is replaced by structurally similar sterols as

the third major constituent of ternary GUVs.[77,78] Indeed, we are aware of four different fluorescently labeled cholesterol molecules whose partitioning between coexisting liquid phases has been investigated: three of these modified cholesterols preferentially segregated into $L_\alpha$ domains, while the fourth enriched in the $L_o$ phase.[79,80] Therefore, the chol-DNAs cannot be assumed to partition in the same proportions as chol between these coexisting phases, since the perturbations in structure of chol-DNA from that of pure chol will have some significance in the molecular insertion into each phase.

We find that the nature of the cholesteryl anchoring geometry affects the partitioning of chol-DNA between coexisting liquid phases. Figure 5A,B shows the partitioning of single-anchored chol-DNA-10A labeled with A647-DNA-10B (blue) between coexisting liquid phases, where the $L_\alpha$ phase is highlighted by inclusion of the Rh-DPPE dye (red). Compare these images to Figure 5C,D where the vesicles are instead functionalized by the double-anchored chol-DNA-20/chol-DNA-30A pair: the single-anchored chol-DNA is seen to partition roughly equally between the two phases, whereas the double-anchored chol-DNA is enriched in the $L_o$ phase compared to the $L_\alpha$ domains.

The relative concentrations of chol-DNA in the two liquid phases can be investigated by quantitative analysis of the fluorescence intensity of A647-DNA-10B in each phase. Figure 6 shows a single confocal image slice through the equator of a 1:1:1 DOPC:DPPC:chol GUV functionalized by double-anchored chol-DNA-20/chol-DNA-30A. We choose to analyze image sections at the equator of the vesicles because, in image sections near the poles of the vesicle, the membrane area per pixel is not constant due to the spherical curvature of the vesicle. A line profile (green) across the vesicle that crosses both the $L_\alpha$ and $L_o$ phases is shown; the intensity profiles as a function of distance along this line section in the two fluorescence channels are shown to the right of the image. From these graphs, the peak intensities of A647-DNA-10B fluorescence can be obtained for each phase, the ratio of which is a measure of the apparent partitioning ($K_p^a$) of chol-DNA between the two phases, i.e., $I_{647}(L_o)/I_{647}(L_\alpha) = K_p^a$, where $I_{647}(L_x)$ is the peak intensity of A647-DNA-10B in the $L_x$ phase.
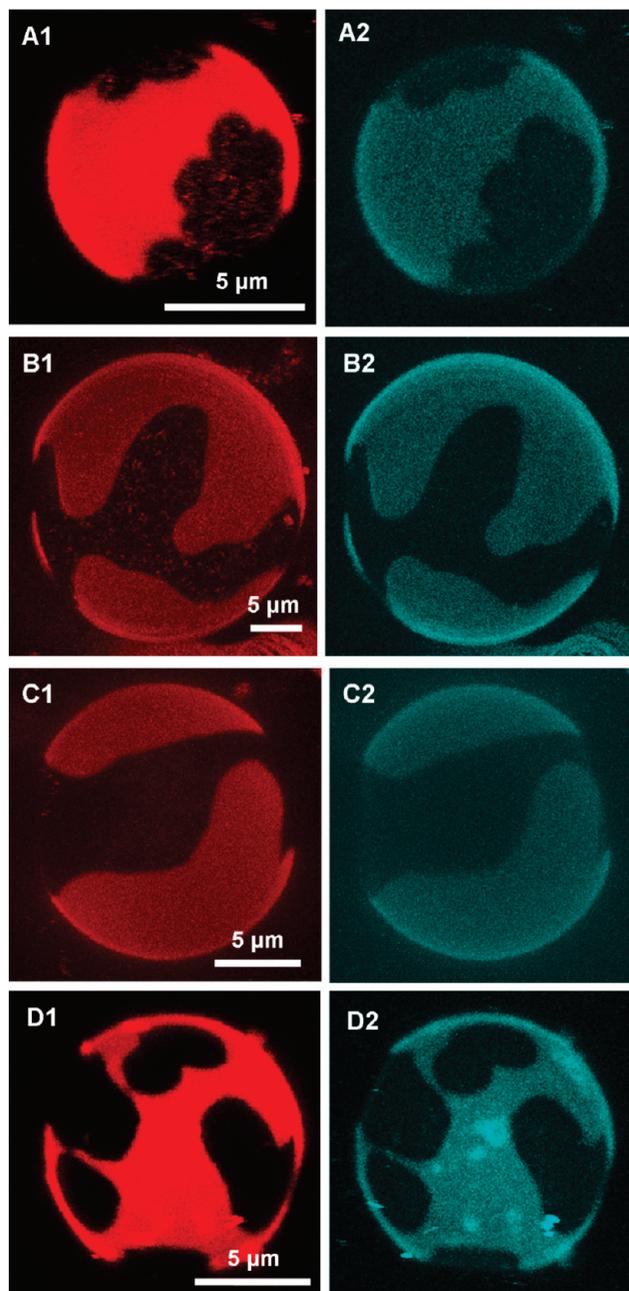
**Figure 4.** Giant vesicles in $L_\alpha$–$L_\beta$ phase coexistence. All vesicles are 1:1 DLPC:DMPE at 21 $\pm$ 1 °C. (A–D) Images are reconstructions of vesicle hemispheres from confocal sections. Images numbered 1 show Rh-DPPE partitioning (the $L_\alpha$ phase), and images numbered 2 show Alexa-647 (DNA) partitioning.

Care must be taken in interpreting relative fluorescence intensities in confocal images, for example, due to possible variations in fluorophore quantum yield between coexisting phases, as has previously been noted.[80] However, in our experiments, the fluorescent probe is extended several nanometers from the bilayer by double-stranded DNA and thus the fluorophore itself will not experience the difference in local membrane environments between coexisting lipid phases; therefore, the local environment of the fluorophore will be the bulk aqueous phase irrespective of which phase the chol-DNA resides in and therefore we do not anticipate any differences in the quantum yield of the probe between phases. Also, we use low chol-DNA concentrations (<1% total lipid concentration) such that we do not anticipate any self-quenching of the fluorescent probe. Probe partitioning between phases is usually

measured by bulk fluorescent spectroscopy experiments. However, for three component systems, the directions of the tie lines within the phase diagram need to be known. Only a few tie lines have been quantitatively reported for this system,[74] and these tie lines have significant error bars such that these errors would hinder the analysis of bulk partitioning data. Therefore, no bulk spectroscopy measurements of the true partitioning coefficients ($K_p$) for chol-DNA between coexisting liquid phases are available to compare with the apparent partitioning ($K_p^a$) we measure from our confocal images. By analyzing several line profiles per vesicle over many vesicles in at least two independent sample preparations, a statistical measurement of the apparent partitioning of chol-DNA between the two phases is obtained.

We quantify the apparent partitioning of the three chol-DNA structures in vesicles of two different lipid compositions in the liquid–liquid coexistence region of DOPC/DPPC/chol membranes (Table 1). The effect of sample history (whether the vesicles were functionalized with DNA before or after phase separation was initiated) does not appear to have a significant effect on the chol-DNA partitioning between phases, since the apparent concentration ratios measured are comparable when taking into account the uncertainty in the data. This is therefore a good indication, but not proof, that we are measuring near-equilibrium partitioning of the chol-DNAs.

Double-chol anchoring of the DNA to the membrane enhances the partitioning of both the chol-DNA-20/chol-DNA-30A and 2p-chol-DNA-10A into the $L_o$ phase compared to that of the single-anchored chol-DNA-10A. This suggests that the two chol moieties per molecule play a significant role in determining the enrichment of these chol-DNAs in the more ordered of the two phases. We do also note that the double-chol moiety is not the sole determinant of the chol-DNA partitioning, since there is a small but significant difference in the apparent partitioning of these two different double-anchored chol-DNA molecules between the liquid phases, where the enrichment of chol-DNA-20/chol-DNA-30A into $L_o$ domains is greatest: other structural factors must fine-tune the exact distribution between the phases. However, our data suggests that the number of cholesterol anchors is the most significant determinant for the observed partitioning. Single-chol-anchored DNA partitions roughly equally between phases with only a small 10–20% apparent enhancement in the $L_o$ phase, whereas enrichment of double-anchored chol-DNA in $L_o$ domains such that the apparent concentration is approximately double that of the $L_\alpha$ phase was achievable in these systems.

The lipid composition of the GUVs also modulates the segregation of the chol-DNAs between phases. The data in Table 1 clearly shows that the enrichment of double-anchored chol-DNAs into the $L_o$ phase is greater for 1:1:1 DOPC:DPPC:chol vesicles than GUVs composed of these lipids in the molar ratio 3:3:2. This is not particularly surprising, since vesicles of a different composition will phase separate along different thermodynamic tie lines, resulting in different compositions for each phase for these two different lipid mixtures. Membrane domains of different lipid compositions will have different properties; for example, increased chol compositions are known to increase rigidity and reduce fluidity of lipid membranes,[81] while these effects are now known not to be universal but dependent on the molecular structure of the lipid(s), e.g., the degree of chain unsaturation, in the membrane into which cholesterol is added.[82] The composition and properties of the domains will therefore determine the exact partitioning of the chol-DNAs between the coexisting phases.

Lipid Phase Partitioning of Anchored DNA

*J. Phys. Chem. B, Vol. 113, No. 42, 2009* **13683**
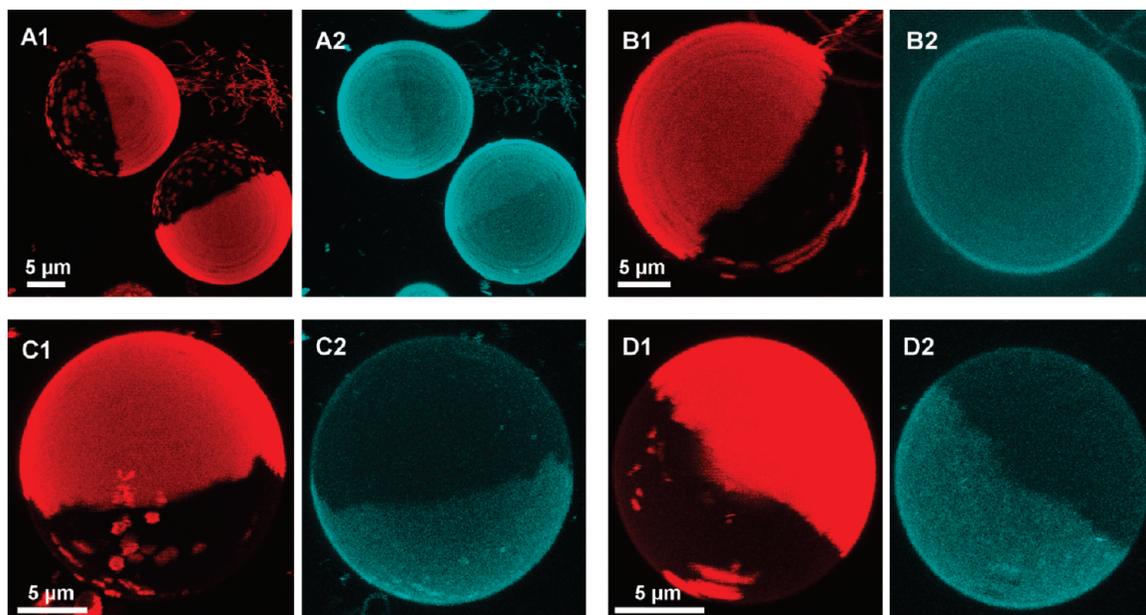


**Figure 5.** Giant vesicles in $L_o$–$L_\alpha$ phase coexistence. All vesicles are 1:1:1 DOPC:DPPC:chol at 21 ± 1 °C. (A–D) Images are reconstructions of vesicle hemispheres from confocal sections. Images numbered 1 show Rh-DPPE partitioning (the $L_\alpha$ phase), and images numbered 2 demonstrate Alexa-647 (DNA probe) partitioning. (A, B) Vesicles are functionalized with single-cholesterol-anchored DNA (chol-DNA-10A). (C, D) Vesicles are functionalized with double-cholesterol-anchored DNA (chol-DNA-30A/chol-DNA-20).
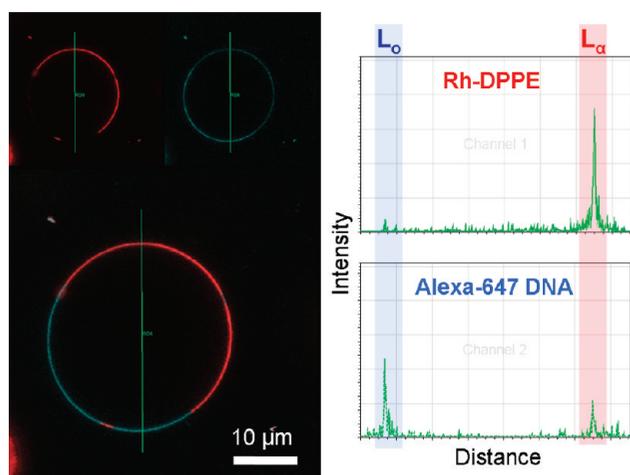


**Figure 6.** (left) Separate fluorescence channels and channel overlay of a confocal slice through the equator of a 1:1:1 DOPC:DPPC:chol vesicle functionalized with double-anchored DNA (chol-DNA-30A/chol-DNA-20) and A647-DNA-10B. Red represents Rh-DPPE (the $L_\alpha$ phase), and blue represents Alexa-647 (DNA probe). The green line represents a line section through the vesicle of which the intensity profiles for each channel are shown (right).

The partitioning of the chol-DNA between lipid domains is determined by the free energy cost of insertion of these molecules into the respective phases. In thermodynamic equilibrium, the concentrations of chol-DNA in each phase are established by $K_p = c(L_o)/c(L_\alpha) = \exp\{-\Delta G(T)/k_B T\}$, where $c(L_x)$ is the concentration of chol-DNA in the $L_x$ phase, $\Delta G(T)$ is the difference in Gibbs free energy for molecular insertion into the two phases, $k_B$ is Boltzmann's constant, and $T$ is the temperature. Therefore, to attempt to understand the enhanced partitioning of the double-anchored chol-DNA in $L_o$ domains, it is necessary to consider how the free energy of insertion into the respective phases might be modulated by having an extra chol anchor.

We propose a simple model based upon the conformational entropy of insertion of a chol anchor into each phase in order

to rationalize the observation that molecules with two anchors partition more strongly into the $L_o$ phase. Pure cholesterol has been measured to partition roughly twice as much into the $L_o$ phase than the $L_\alpha$ phase for 1:1 DOPC:DPPC vesicles with 30% chol at 25 °C,[74] demonstrating a lower chemical potential for molecular insertion of cholesterol into the $L_o$ phase (it should be noted however that the exact quantitative partitioning of chol between coexisting phases will depend on the particular tie line along which the vesicle phase separates, i.e., the specific temperature and membrane composition). The single-anchored chol-DNA still shows a slight apparent enhancement in the $L_o$ phase by around 10−20% which implies that this molecule has a lower free energy benefit for partitioning into the $L_o$ phase than pure chol. This is likely to be due to the free energy cost due to the imposition of the TEG linker to the DNA strand through the headgroup region of the membrane being greater in the more ordered $L_o$ phase, although we cannot discount an additional energy cost due to the rigid double-stranded DNA that extends into the aqueous phase outside of the lipid bilayer.

The preference of chol to partition more strongly into the DPPC-rich $L_o$ phase as opposed to the DOPC-rich $L_\alpha$ phase is thought to be at least partially due to the difficulty of insertion of the rigid fused-ring structure of the sterol next to the unsaturated acyl chains of the DOPC, which cause its hydrophobic tails to kink. This is exemplified by the finding that chol prefers to lie flat in the center of membranes composed of highly unsaturated lipids as opposed to its usual "upright" location with the hydroxyl group situated near the amphiphilic interface with hydrophilic headgroups of the lipids.[83,84] This unfavorability of locating the chol moiety next to the unsaturated DOPC will reduce the number of possible conformations that chol can insert into the $L_\alpha$ phase compared to the $L_o$ domains. If we assume that the chol anchor can insert $n$ ways into the $L_\alpha$ phase and $qn$ ways into the $L_o$ phase, where $q$ (>1) represents the proportional increase in possible conformations that the chol anchor can insert into the $L_o$ phase than the $L_\alpha$ phase, then the conformational entropy difference between insertion into the two phases for a single-cholesterol anchor is $\Delta S_{single} \propto \ln q$. In the case of two

**TABLE 1: Ratio of the Average Fluorescence Intensities from A647-DNA-10B in Coexisting Liquid Phases, $I(L_o)/I(L_\alpha)$, for Different GUV Compositions, Sample Histories, and Hydrophobic Anchoring Geometries**

| membrane-anchored DNA | 1:1:1 DOPC:DPPC:chol | | 3:3:2 DOPC:DPPC:chol | |
| | chol-DNA added *before* phase separation | chol-DNA added *after* phase separation | chol-DNA added *before* phase separation | chol-DNA added *after* phase separation |
| --- | --- | --- | --- | --- |
| single anchor (chol-DNA-10A) | $1.32 \pm 0.10$ | $1.19 \pm 0.09$ | $1.12 \pm 0.05$ | $1.18 \pm 0.08$ |
| double anchor (chol-DNA-20/ chol-DNA-30A) | $1.94 \pm 0.16$ | $2.09 \pm 0.17$ | $1.68 \pm 0.14$ | $1.76 \pm 0.14$ |
| double anchor (2p-chol-DNA-10A) | $1.78 \pm 0.13$ | $1.98 \pm 0.11$ | $1.56 \pm 0.07$ | $1.66 \pm 0.07$ |

chol anchors per molecule, we can make the first order assumption that the number of ways each chol can insert into each phase is not influenced by being tethered to each other; i.e., the conformational freedom of two chol anchors for insertion into each phase is not coupled. Then, for the $L_\alpha$ phase, the first chol anchor can insert $n$ ways into the phase and the second chol anchor can also insert in $n$ ways at a nearby location in this phase, such that the double-anchored molecule can insert in $n^2$ ways into the $L_\alpha$ phase. Similarly, for the $L_o$ phase, the double-chol-anchored molecule can then insert in $q^2 n^2$ ways, resulting in a conformational entropy difference for molecular insertion into the two phases of $\Delta S_{double} \propto 2 \ln q$. Therefore, the difference in conformational entropy gain for insertion into the $L_o$ phase, $\Delta\Delta S = \Delta S_{double} - \Delta S_{single} \propto \ln q$, means that there is an increase in conformational entropy gain for insertion of the double-chol-anchored DNA into the $L_o$ phase, thereby enhancing this molecule's partitioning into these domains.

We note that if there is some coupling between the two chol moieties due to being tethered together into the same molecule such that insertion of the first anchor restricts the number of conformations by which the second can insert, then $\Delta S_{double} \propto r \ln q$, where $1 < r < 2$; this still predicts an enhanced partitioning of the double-anchored chol-DNA into the $L_o$ phase compared to that of the single-chol variant. Indeed, a difference in such a coupling between the chol moieties of the chol-DNA-20/chol-DNA-30A and 2p-chol-DNA-10A due to the details of their linker chemistry could explain the slight differences in partitioning observed for these molecules; the first three bases of the chol-DNA-20/chol-DNA-30A are noncomplementary and hence do not hybridize, which is likely to reduce any conformational coupling effects between the two chol anchors for this molecule.

While this very simple model based upon changes in molecular conformational entropy predicts the phenomenon of enhanced partitioning of the double-anchored chol-DNA into the $L_o$ domains, a full thermodynamic description of the observed partitioning would involve consideration of the both entropic and enthalpic contributions to the free energy of insertion. Formulation of such a model is likely to be challenging, since cholesterol−lipid interactions are known to be complex. These interactions are known to be sensitive to the specific structure of the lipids,[82] and several models exist for the molecular behavior of chol in lipid phases, including the "umbrella model"[85] and models based upon the formation of condensed lipid−chol complexes.[82,86,87]

The enrichment of the double-anchored DNA molecules in the $L_o$ domains could be used to create selectively sticky patches on the vesicle surface. Figure 7 shows a liquid−liquid phase-separated GUV functionalized with chol-DNA-20/chol-DNA-30A; note that the morphology of the domains in these vesicles ripens to a single domain by coalescence, reducing the line tension between phases. This two-faced texture is analogous to that of "Janus particles".[88] We have previously reported a phase diagram for GUV binding mediated by DNA functionalization with varying DNA surface concentration and solution ionic

strength,[27] where the precise quantitative location of the phase boundaries will also be dependent on the DNA sequence used. A cartoon of such a phase diagram is illustrated in the bottom right of Figure 7; the phase boundary drawn indicates a transition between no vesicle adhesion and vesicle adhesion mediated by specific binding of cDNA sequences. Since double-anchored chol-DNAs show an apparent enrichment to approximately twice the surface concentration in the $L_o$ phase compared to the $L_\alpha$ phase, the system could be engineered such that the DNA concentration in the $L_o$ phase favors adhesion and the concentration in the $L_\alpha$ phase does not, as shown in Figure 7. This would break the spherical symmetry of intervesicle interactions, introducing directional binding. Experimental realization and investigation of preferential adhesion between the $L_o$ domains of such vesicles will be a subject of future work in our lab. Furthermore, introducing a second DNA sequence with a different hydrophobic modification which anchors the DNA preferentially in the $L_\alpha$ phase would allow fabrication of domains functionalized by different nucleic acid sequences. Such a modification has been reported by Bunge et al.[6,9] Investigation of the phase partitioning of different hydrophobic modifications for DNA will provide a toolbox for the fabrication of multi-
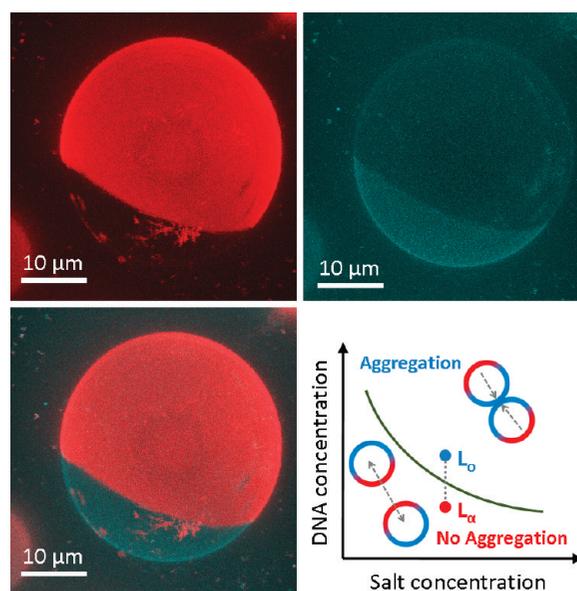


**Figure 7.** Selectively sticky DNA domains on liquid−liquid phase-separated GUVs. 1:1:1 DOPC:DPPC:chol GUV functionalized with chol-DNA-20/chol-DNA-30A: Rh-DPPE emission (top left), A647-DNA-10B emission (top right), composite image (bottom left). (bottom right) Cartoon of a phase diagram for DNA-functionalized GUVs with varying DNA surface concentration and solution ionic strength based on the phase diagram in ref 20. DNA partitioning in phase-separated GUVs could be engineered such that only the DNA surface concentration in the $L_o$ phase is high enough for binding with complementary sequences at the solution ionic strength (as shown by the data points signifying DNA concentrations in the two phases: one above and one below the phase boundary for vesicle aggregation).

functional textured vesicles tailored for specific technological applications.

## Summary

We have investigated the partitioning of different hydrophobically modified DNAs based upon cholesterol anchoring between different coexisting lipid phases. All chol-DNAs tested were essentially excluded from solid-like lipid domains that formed in fluid vesicle membranes irrespective of the specific molecular packing structure of the solid phase. Partitioning of chol-DNAs between coexisting liquid domains was found to be more complex with a detectable fluorescence signal in each phase due to the localization of the chol-DNA within the membrane. The quantitative apparent partitioning of the chol-DNA is seen to be dependent on the details of the molecular structure of the chol-DNA and the precise lipid composition of the coexisting domains. The most significant modulation of chol-DNA partitioning is observed when two cholesterol anchors are used instead of a single-chol moiety: double-chol anchoring enhanced the chol-DNA partitioning into the $L_o$ phase. We interpret this observation in terms of the conformational entropy of insertion of a chol anchor into each phase, where the rigid sterol structure can access fewer conformational states due to the "kinks" in the acyl chains of DOPC in the $L_\alpha$ phase. These results demonstrate that lipid phase separation is an effective tool to engineer asymmetric distributions of anchored DNA molecules on a vesicle surface. Vesicle domains encoded with information in the form of anchored nucleic acid sequences may fill roles as intelligent, soft containers in biotechnology.

## References and Notes

(1) Liu, X. D.; Yamada, M.; Matsunaga, M.; Nishi, N. Functional materials derived from DNA. In *Functional Materials and Biomaterials*; Springer-Verlag: Berlin, 2007; Vol. 209, p 149.

(2) Krieg, A. M.; Tonkinson, J.; Matson, S.; Zhao, Q. Y.; Saxon, M.; Zhang, L. M.; Bhanja, U.; Yakubov, L.; Stein, C. A. *Proc. Natl. Acad. Sci. U.S.A.* **1993**, *90*, 1048.

(3) Ajo-Franklin, C. M.; Yoshina-Ishii, C.; Boxer, S. G. *Langmuir* **2005**, *21*, 4976.

(4) Benkoski, J. J.; Hook, F. *J. Phys. Chem. B* **2005**, *109*, 9773.

(5) Benkoski, J. J.; Jesorka, A.; Edvardsson, M.; Hook, F. *Soft Matter* **2006**, *2*, 710.

(6) Bunge, A.; Kurz, A.; Windeck, A. K.; Korte, T.; Flasche, W.; Liebscher, J.; Herrmann, A.; Huster, D. *Langmuir* **2007**, *23*, 4455.

(7) Dahlin, A. B.; Jonsson, M. P.; Hook, F. *Adv. Mater.* **2008**, *20*, 1436.

(8) Gunnarsson, A.; Jonsson, P.; Marie, R.; Tegenfeldt, J. O.; Hook, F. *Nano Lett.* **2008**, *8*, 183.

(9) Kurz, A.; Bunge, A.; Windeck, A. K.; Rost, M.; Flasche, W.; Arbuzova, A.; Strohbach, D.; Mueller, S.; Liebscher, J.; Huster, D.; Herrmann, A. *Angew. Chem., Int. Ed.* **2006**, *45*, 4440.

(10) Pfeiffer, I.; Hook, F. *J. Am. Chem. Soc.* **2004**, *126*, 10224.

(11) Stadler, B.; Falconnet, D.; Pfeiffer, I.; Hook, F.; Voros, J. *Langmuir* **2004**, *20*, 11348.

(12) Svedhem, S.; Pfeiffer, I.; Larsson, C.; Wingren, C.; Borrebaeck, C.; Hook, F. *ChemBioChem* **2003**, *4*, 339.

(13) Yoshina-Ishii, C.; Boxer, S. G. *J. Am. Chem. Soc.* **2003**, *125*, 3696.

(14) Yoshina-Ishii, C.; Boxer, S. G. *Langmuir* **2006**, *22*, 2384.

(15) Yoshina-Ishii, C.; Chan, Y. H. M.; Johnson, J. M.; Kung, L. A.; Lenz, P.; Boxer, S. G. *Langmuir* **2006**, *22*, 5682.

(16) Yoshina-Ishii, C.; Miller, G. P.; Kraft, M. L.; Kool, E. T.; Boxer, S. G. *J. Am. Chem. Soc.* **2005**, *127*, 1356.

(17) Gissot, A.; Camplo, M.; Grinstaff, M. W.; Barthelemy, P. *Org. Biomol. Chem.* **2008**, *6*, 1324.

(18) Dusseiller, M. R.; Niederberger, B.; Stadler, B.; Falconnet, D.; Textor, M.; Voros, J. *Lab Chip* **2005**, *5*, 1387.

(19) Stadler, B.; Bally, M.; Grieshaber, D.; Voros, J.; Brisson, A.; Grandin, H. M. *Biointerphases* **2006**, *1*, 142.

(20) Grosser, S. T.; Savard, J. M.; Schneider, J. W. *Anal. Chem.* **2007**, *79*, 9513.

(21) Lau, C.; Bitton, R.; Bianco-Peled, H.; Schultz, D. G.; Cookson, D. J.; Grosser, S. T.; Schneider, J. W. *J. Phys. Chem. B* **2006**, *110*, 9027.

(22) Marques, B. F.; Schneider, J. W. *Langmuir* **2005**, *21*, 2488.

(23) Savard, J. M.; Schneider, J. W. *Biotechnol. Bioeng.* **2007**, *97*, 367.

(24) Vernille, J. P.; Kovell, L. C.; Schneider, J. W. *Bioconjugate Chem.* **2004**, *15*, 1314.

(25) Dentinger, P. M.; Simmons, B. A.; Cruz, E.; Sprague, M. *Langmuir* **2006**, *22*, 2935.

(26) Gissot, A.; Di Primo, C.; Bestel, I.; Giannone, G.; Chapuis, H.; Barthelemy, P. *Chem. Commun.* **2008**, 5550.

(27) Beales, P. A.; Vanderlick, T. K. *J. Phys. Chem. A* **2007**, *111*, 12372.

(28) Chan, Y. H. M.; Lenz, P.; Boxer, S. G. *Proc. Natl. Acad. Sci. U.S.A.* **2007**, *104*, 18913.

(29) Beales, P. A.; Vanderlick, T. K. *Biophys. J.* **2009**, *96*, 1554.

(30) Chan, Y.-H. M.; van Lengerich, B.; Boxer, S. G. *Biointerphases* **2008**, *3*, FA17.

(31) Stengel, G.; Simonsson, L.; Campbell, R. A.; Hook, F. *J. Phys. Chem. B* **2008**, *112*, 8264.

(32) Stengel, G.; Zahn, R.; Hook, F. *J. Am. Chem. Soc.* **2007**, *129*, 9584.

(33) Rothemund, P. W. K. *Nature* **2006**, *440*, 297.

(34) Seeman, N. C.; Lukeman, P. S. *Rep. Prog. Phys.* **2005**, *68*, 237.

(35) Bath, J.; Turberfield, A. J. *Nat. Nanotechnol.* **2007**, *2*, 275.

(36) Chen, Y.; Lee, S. H.; Mao, C. *Angew. Chem., Int. Ed.* **2004**, *43*, 5335.

(37) Ferapontova, E. E.; Mountford, C. P.; Crain, J.; Buck, A. H.; Dickinson, P.; Beattie, J. S.; Ghazal, P.; Terry, J. G.; Walton, A. J.; Mount, A. R. *Biosens. Bioelectron.* **2008**, *24*, 422.

(38) Liu, D. S.; Bruckbauer, A.; Abell, C.; Balasubramanian, S.; Kang, D. J.; Klenerman, D.; Zhou, D. J. *J. Am. Chem. Soc.* **2006**, *128*, 2067.

(39) Mao, C. D.; Sun, W. Q.; Shen, Z. Y.; Seeman, N. C. *Nature* **1999**, *397*, 144.

(40) Han, X. G.; Zhou, Z. H.; Yang, F.; Deng, Z. X. *J. Am. Chem. Soc.* **2008**, *130*, 14414.

(41) Yurke, B.; Turberfield, A. J.; Mills, A. P.; Simmel, F. C.; Neumann, J. L. *Nature* **2000**, *406*, 605.

(42) Sherman, W. B.; Seeman, N. C. *Nano Lett.* **2004**, *4*, 1203.

(43) Shin, J. S.; Pierce, N. A. *J. Am. Chem. Soc.* **2004**, *126*, 10834.

(44) Yin, P.; Yan, H.; Daniell, X. G.; Turberfield, A. J.; Reif, J. H. *Angew. Chem., Int. Ed.* **2004**, *43*, 4906.

(45) Proske, D.; Blank, M.; Buhmann, R.; Resch, A. *Appl. Microbiol. Biotechnol.* **2005**, *69*, 367.

(46) Patil, S. D.; Rhodes, D. G.; Burgess, D. J. *Biochim. Biophys. Acta* **2005**, *1711*, 1.

(47) Cheng, J.; Teply, B. A.; Sherifi, I.; Sung, J.; Luther, G.; Gu, F. X.; Levy-Nissenbaum, E.; Radovic-Moreno, A. F.; Langer, R.; Farokhzad, O. C. *Biomaterials* **2007**, *28*, 869.

(48) Chu, T. C.; Twu, K. Y.; Ellington, A. D.; Levy, M. *Nucleic Acids Res.* **2006**, 34.

(49) Farokhzad, O. C.; Cheng, J. J.; Teply, B. A.; Sherifi, I.; Jon, S.; Kantoff, P. W.; Richie, J. P.; Langer, R. *Proc. Natl. Acad. Sci. U.S.A.* **2006**, *103*, 6315.

(50) Farokhzad, O. C.; Jon, S. Y.; Khadelmhosseini, A.; Tran, T. N. T.; LaVan, D. A.; Langer, R. *Cancer Res.* **2004**, *64*, 7668.

(51) Forssen, E.; Willis, M. *Adv. Drug Delivery Rev.* **1998**, *29*, 249.

(52) Bagatolli, L. A.; Gratton, E. *Biophys. J.* **2000**, *79*, 434.

(53) Bagatolli, L. A.; Gratton, E. *Biophys. J.* **2000**, *78*, 290.

(54) Beales, P. A.; Gordon, V. D.; Zhao, Z. J.; Egelhaaf, S. U.; Poon, W. C. K. *J. Phys.: Condens. Matter* **2005**, *17*, S3341.

(55) Gordon, V. D.; Beales, P. A.; Shearman, G. C.; Zhao, Z.; Seddon, J. M.; Egelhaaf, S. U.; Poon, W. C. K. *Phys. Rev. E*, submitted for publication, 2009.

(56) Gordon, V. D.; Beales, P. A.; Zhao, Z.; Blake, C.; MacKintosh, F. C.; Olmsted, P. D.; Cates, M. E.; Egelhaaf, S. U.; Poon, W. C. K. *J. Phys.: Condens. Matter* **2006**, *18*, L415.

(57) Korlach, J.; Schwille, P.; Webb, W. W.; Feigenson, G. W. *Proc. Natl. Acad. Sci. U.S.A.* **1999**, *96*, 8461.

(58) Feigenson, G. W.; Buboltz, J. T. *Biophys. J.* **2001**, *80*, 2775.

(59) Baumgart, T.; Hess, S. T.; Webb, W. W. *Nature* **2003**, *425*, 821.

(60) Scherfeld, D.; Kahya, N.; Schwille, P. *Biophys. J.* **2003**, *85*, 3758.

(61) Veatch, S. L.; Keller, S. L. *Phys. Rev. Lett.* **2002**, *89*, 4.

(62) Veatch, S. L.; Keller, S. L. *Biophys. J.* **2003**, *85*, 3074.

(63) Yang, S. M.; Kim, S. H.; Lim, J. M.; Yi, G. R. *J. Mater. Chem.* **2008**, *18*, 2177.

(64) Nelson, E. C.; Braun, P. V. *Science* **2007**, *318*, 924.

(65) Paxton, W. F.; Sundararajan, S.; Mallouk, T. E.; Sen, A. *Angew. Chem., Int. Ed.* **2006**, *45*, 5420.

(66) Dietrich, C.; Bagatolli, L. A.; Volovyk, Z. N.; Thompson, N. L.; Levi, M.; Jacobson, K.; Gratton, E. *Biophys. J.* **2001**, *80*, 1417.

(67) Edidin, M. *Annu. Rev. Biophys. Biomol. Struct.* **2003**, *32*, 257.

(68) Jacobson, K.; Mouritsen, O. G.; Anderson, R. G. W. *Nat. Cell Biol.* **2007**, *9*, 7.

(69) Simons, K.; Vaz, W. L. C. *Annu. Rev. Biophys. Biomol. Struct.* **2004**, *33*, 269.

(70) Hancock, J. F. *Nat. Rev. Mol. Cell Biol.* **2006**, 7, 456.

(71) Brown, D. A.; London, E. *Annu. Rev. Cell Dev. Biol.* **1998**, *14*, 111.

(72) Simons, K.; Toomre, D. *Nat. Rev. Mol. Cell Biol.* **2000**, *1*, 31.

(73) Mart, R. J.; Liem, K. P.; Wang, X.; Webb, S. J. *J. Am. Chem. Soc.* **2006**, *128*, 14462.

(74) Veatch, S. L.; Polozov, I. V.; Gawrisch, K.; Keller, S. L. *Biophys. J.* **2004**, *86*, 2910.

(75) Scheidt, H. A.; Muller, P.; Herrmann, A.; Huster, D. *J. Biol. Chem.* **2003**, *278*, 45563.

(76) Wustner, D. *Chem. Phys. Lipids* **2007**, *146*, 1.

(77) Beattie, M. E.; Veatch, S. L.; Stottrup, B. L.; Keller, S. L. *Biophys. J.* **2005**, *89*, 1760.

(78) Bacia, K.; Schwille, P.; Kurzchalia, T. *Proc. Natl. Acad. Sci. U.S.A.* **2005**, *102*, 3272.

(79) Baumgart, T.; Hunt, G.; Farkas, E. R.; Webb, W. W.; Feigenson, G. W. *Biochim. Biophys. Acta* **2007**, *1768*, 2182.

(80) Sengupta, P.; Hammond, A.; Holowka, D.; Baird, B. *Biochim. Biophys. Acta* **2008**, *1778*, 20.

(81) Henriksen, J.; Rowat, A. C.; Brief, E.; Hsueh, Y. W.; Thewalt, J. L.; Zuckermann, M. J.; Ipsen, J. H. *Biophys. J.* **2006**, *90*, 1639.

(82) Pan, J. J.; Mills, T. T.; Tristram-Nagle, S.; Nagle, J. F. *Phys. Rev. Lett.* **2008**, *100*.

(83) Harroun, T. A.; Katsaras, J.; Wassall, S. R. *Biochemistry* **2008**, *47*, 7090.

(84) Marrink, S. J.; de Vries, A. H.; Harroun, T. A.; Katsaras, J.; Wassall, S. R. *J. Am. Chem. Soc.* **2008**, *130*, 10.

(85) Huang, J. Y.; Feigenson, G. W. *Biophys. J.* **1999**, *76*, 2142.

(86) Hung, W. C.; Lee, M. T.; Chen, F. Y.; Huang, H. W. *Biophys. J.* **2007**, *92*, 3960.

(87) McConnell, H.; Radhakrishnan, A. *Proc. Natl. Acad. Sci. U.S.A.* **2006**, *103*, 1184.

(88) Walther, A.; Muller, A. H. E. *Soft Matter* **2008**, *4*, 663.